**ORIGINAL PAPER**

# Liraglutide Alleviates Cognitive Deficit in db/db Mice: Involvement in Oxidative Stress, Iron Overload, and Ferroptosis

Ji-Ren An[1] · Jia-Nan Su[1] · Gui-Yan Sun[1] · Qing-Feng Wang[1] · Ya-Dong Fan[2] · Nan Jiang[1] · Yu-Feng Yang[1] · Yan Shi[1]

## Abstract
Studies have shown that diabetes is associated with the occurrence of neurodegenerative diseases and cognitive decline. However, there is currently no effective treatment for diabetes-induced cognitive dysfunction. The superior efficacy of liraglutide (LIRA) for cognitive impairment and numerous neurodegenerative diseases has been widely demonstrated. This study determined the effects of LIRA on diabetic cognitive impairment and on the levels of oxidative stress, lipid peroxidation, iron metabolism and ferroptosis in the hippocampus. Mice were injected daily with liraglutide (200 µg/kg/d) for 5 weeks. LIRA could repair damaged neurons and synapses, and it increased the protein expression levels of PSD 95, SYN, and BDNF. Furthermore, LIRA significantly decreased oxidative stress and lipid peroxidation levels by downregulating the production of ROS and MDA and upregulating SOD and GSH-Px in the serum and hippocampus, and the upregulation of SOD2 expression was also proven. The decreased levels of TfR1 and the upregulation of FPN1 and FTH proteins observed in the LIRA-treated db/db group were shown to reduce iron overload in the hippocampus, whereas the increased expression of Mtft and decreased expression of Mfrn in the mitochondria indicated that mitochondrial iron overload was ameliorated. Finally, LIRA was shown to prevent ferroptosis in the hippocampus by elevating the expression of GPX4 and SLC7A11 and suppressing the excessive amount of ACSL4; simultaneously, the damage to the mitochondria observed by TEM was also repaired. For the first time, we proved in the T2DM model that ferroptosis occurs in the hippocampus, which may play a role in diabetic cognitive impairment. LIRA can reduce oxidative stress, lipid peroxidation and iron overload in diabetic cognitive disorders and further inhibit ferroptosis, thereby weakening the damage to hippocampal neurons and synaptic plasticity and ultimately restoring cognitive function.

**Keywords** Diabetic cognitive impairment · Liraglutide · Ferroptosis · Iron overload · Oxidative stress

Ji-Ren An and Jia-Nan Su have contributed equally to this work and share first authorship.

✉ Yu-Feng Yang
  lntcmyyf@126.com

✉ Yan Shi
  lntcmshiyan@163.com

1 Liaoning University of Traditional Chinese Medicine, Huanggu District, No. 79, Mount Chong East Road, Shenyang 110847, China

2 Tianjin University of Traditional Chinese Medicine, Tianjin 301617, China

## Introduction

Diabetes mellitus is one of the most common metabolic disorders and is characterized by elevated blood glucose resulting from a deficiency in insulin secretion or insulin resistance [1]. The global incidence of diabetes mellitus is increasing rapidly and has become a worldwide public health issue threatening human health. In addition to diabetes-related microvascular and macrovascular complications, concurrent neurobehavioral defects pose additional challenges to treatment. A number of experimental and clinical reports suggest that type 2 diabetes mellitus (T2DM) occurs simultaneously with brain diseases such as Alzheimer's disease, depression, and cognitive impairment [2–4]. Diabetes mellitus is intricately linked to cognitive impairment [5], and approximately 50% of T2DM patients suffer from cognitive dysfunction [6].

Ferroptosis, a regulated, nonapoptotic form of iron-dependent cell death, was first proposed in 2012 and is defined as the inactivation of phospholipid hydroperoxidase glutathione peroxidase 4 (GPX4) with the occurrence of iron-dependent lipid peroxidation [7, 8]. The labile iron pool promotes ferroptosis by catalyzing the production of a large amount of reactive oxygen species (ROS), which provides a powerful oxidant for lipid peroxidation [9]. Iron overload is a key factor in ferroptosis, which is supported by the results of iron-chelating agents in reducing ferroptosis in multiple experimental models [7, 10]. Ferroptosis has been proven to participate in diverse pathological cell deaths in numerous degenerative pathologies [11]. A recent study found that ferroptosis of brain microvascular endothelial cells occurs after diabetic stroke, and iron-chelating agents can effectively inhibit the occurrence of endothelial ferroptosis and vascular degeneration, which is undoubtedly a strong link between ferroptosis and diabetic brain damage [12]. However, the role of ferroptosis in diabetic cognitive impairment and hippocampal lesions is yet to be fully defined.

Previous research has found that approximately 1/10 of cases of Alzheimer's disease are attributed to the aggravation of diabetes[13], while T2DM patients exhibit AD-like brain pathological changes [14]. However, current therapies have limited efficacy against diabetic cognitive impairment. Therefore, the cognitive impairment caused by diabetes will gradually progress and may evolve into a more serious neurodegenerative disease. As such, there is an urgent need for the exploration of new therapeutic strategies aimed at targeting diabetic cognitive impairment.

Glucagon-like peptide-1 (GLP-1) is a peptide hormone that stimulates insulin secretion and inhibits glucagon secretion in the pancreas in a glucose-dependent manner [15]. Liraglutide (LIRA), a GLP-1 receptor agonist, is currently widely used in the clinic and is approved for the treatment of obesity and diabetes. Previous studies have found that liraglutide can significantly improve the blood glucose level compared with other GLP-1 receptor agonists [16]. Beyond that, LIRA has been identified to have a neuroprotective effect on nerves and cognition. LIRA can reduce Aβ deposition and glial cell activation in the cortex and hippocampus of Alzheimer's disease mice [17]. In addition, LIRA is good at reducing the level of phosphorylated tau in cultured neurons and mice and mitigating the loss of hippocampal neurons in Alzheimer's disease mice [18]. LIRA not only has a hypoglycemic effect but also has been proven to be related to a variety of regulatory processes, such as oxidative stress [19]. However, the fundamental cellular mechanism of LIRA agonists involved in the brain remains poorly understood.

In view of this, we hope to solve the above problems by establishing a db/db mouse diabetes model, which is widely used in the study of T2DM and related complications [20]. First, to evaluate the changes in glucose and lipid metabolism in mice, we tested weekly blood glucose, glucose tolerance, insulin tolerance, pyruvate tolerance, total cholesterol, triglycerides, low-density lipoprotein, and insulin levels. After that, we conducted a Morris water maze experiment and a Y maze experiment to study the influence of the model on behavior. At the same time, we observed changes in neurons and synapses in the hippocampus through Nissl staining and transmission electron microscopy, accompanied by PSD95, SYN and BDNF detection of protein expression. We further tested the levels of antioxidants (SOD and GSH-Px) and lipid peroxidation products (MDA) in the serum and hippocampus and performed DHE staining to observe the changes in reactive oxygen species. Perls' staining was used to observe iron deposition in the hippocampus. At the same time, western blotting was used to detect the expression of the iron-related proteins FTL, FTH, TfR1, and FPN1 and mitochondrial iron storage protein FtMt and uptake protein Mfrn. Morphological changes in mitochondria were observed by transmission electron microscopy. Finally, immunofluorescence and western blotting were used to detect the expression levels of ACSL4, SLC7A11 and GPX4 in the ferroptosis signal transduction pathway. Here, our purpose was to evaluate whether ferroptosis plays a role in the pathogenesis of neuronal damage caused by T2DM, and to determine the effect of LIRA, with the aim of providing potential therapeutic targets.

## Materials and Methods

### Experimental Animals and Grouping

Male diabetic db/db mice and nondiabetic littermate db/m mice that were 4 weeks of age were purchased from Changzhou Cavens Experimental Animal Co., Ltd. (Changzhou, China). All mice were adapted to their living conditions for at least 7 days before the experiment. After 1 week of adaptive feeding, 20 db/db mice were randomly divided into two groups: a model group (db/db, n = 10) and a treatment group (LIRA, n = 10). Another 10 db/m mice were used as the control group (db/m, n = 10). After feeding to 10 weeks old, the LIRA group was given liraglutide (CSN11311, CSNpharm, China) diluent (200 μg/kg/d) by intraperitoneal injection for 5 weeks, with equivoluminal 0.9% saline intraperitoneally administered to the other two groups. During the experiment, the tail veins of the mice were massaged and disinfected with 75% ethanol, followed by puncture and collection of 1 drop of blood, and the blood glucose levels were measured by a blood glucose meter (S59400839789, Sannuo, China) per week. All mice were allowed free access to food and water.

After the experiment, the mice were anesthetized, and blood was collected. The hippocampal regions of the brains

were obtained and examined by transmission electron microscopy, histology, Western blot, immunohistochemistry and immunofluorescence.

All procedures were carried out in strict accordance with the National Institutes of Health Guide for the Care and Use of Laboratory Animals and were approved by the Animal Experimental Ethics Committee of Liaoning University of Traditional Chinese Medicine (Ethics approval number: SYXK 2019–0004).

## Intraperitoneal Injection of Glucose, Insulin and Pyruvate Tolerance Test

An intraperitoneal glucose tolerance test (IPGTT) was first performed three days prior to harvesting, and then an intraperitoneal insulin tolerance test (IPITT) was performed to evaluate systemic glucose tolerance and insulin sensitivity. Mice were injected with glucose (2 g/kg) or insulin (1 U/kg) in the awake state and were then fasted for 12 h (since 7 a.m.), and blood glucose levels were measured by tail bleeding at each time point indicated. Finally, an intraperitoneal pyruvate tolerance test (IPPTT) was performed by intraperitoneal injection of mice with pyruvate. After fasting for 14 h, the mice were injected with sodium pyruvate (2 g/kg), and then the blood glucose levels at each time point were measured by tail hemorrhage. The area under the curve (AUC) of blood glucose fluctuation was also calculated.

## Behavioral Experiment

The Morris water maze test (MWM) is widely used to test memory function and was performed as described previously [21]. The MWM test was performed with the SMART-CS (Panlab, Barcelona, Spain) program. On the 1st day, the platform was placed above the water surface (visible platform) for memory training. From the 2nd to the 6th day, the platform was placed just below the water surface (hidden platform) for the site navigation test. Each mouse was placed in the tank from one of four different directions, and the distance traveled and latency to reach the platform were recorded. On the 7th–9th day, the platform was placed in the opposite area and continued to be placed just below the water surface to repeat the field navigation test. On the 10th day, the platform was removed for the probe trial. The number of times the platform location was crossed within 2 min was recorded.

The Y maze was used to test the discriminative learning and working memory of the mice. The Y maze consists of three identical zones, named the starting zone, the new zone and the other zone. In the first experiment, the new zone was first closed, and the mice were placed in the maze and allowed 3 min of free exploration. The second experiment (recall stage) was conducted after 2 h of waiting. The new zone was opened, and the mice were allowed to freely explore the three arms for 3 min. The ratio of exploration time and distance in each zone was recorded. The time and distance for mice with cognitive impairment to explore in the new zone would be shortened.

## Nissl Staining

Nissl staining was used to detect the number and morphology of Nissl bodies in hippocampal neurons. After the brain tissues were removed, they were sliced into 5-μm paraffin sections by a vibrating slicer (CM1950, Leica, Solms, Germany). The slices were deparaffinized, rehydrated, stained with Nissl staining, dehydrated, and made transparent. Finally, the brain slices were covered and photographed by electron microscopy (DM3000, Leica, Sims, Germany).

## Transmission Electron Microscope (TEM) Staining

We used a blade to cut and harvest fresh hippocampal tissue blocks quickly that were no more than 1 mm$^3$. The removed tissue was immediately placed into a fixative for TEM (G1102, Servicebio, Wuhan, China) and was fixed at 4 °C for preservation. Then, the tissues were washed using 0.1 M PBS (pH 7.4) 3 times, 15 min each. Pure EMBed 812 (90,529–77–4, SPI, USA) was poured into the embedding models, and the tissues were inserted into pure EMBed 812 and then kept in 37 °C ovens overnight. The embedding models with resin and samples were moved into 65℃ ovens to polymerize for more than 48 h. Then, the resin blocks were cut to 60–880-nm-thick sections on an ultramicrotome, and the tissues were removed onto 150-mesh cuprum grids with formvar film. The sections were stained in a 2% uranyl acetate saturated alcohol solution for 8 min in the dark, rinsed with 70% ethanol 3 times, and rinsed with ultrapure water three times. The sections were stained in a 2.6% lead citrate solution to avoid carbon dioxide for 8 min and washed with ultrapure water 3 times, and the filter paper was slightly blotted dry. The cuprum grids were placed in a copper mesh box and dried overnight at room temperature. The cuprum grids were observed under TEM, and images were taken.

## Serum Analysis

Serum total cholesterol (TC) and low-density lipoprotein (LDL) were measured using a biochemical kit (2,020,002, Huili Biotech Co., Ltd, Changchun, China); triglyceride (TG) was determined using a biochemical kit (2,020,008, Huili Biotech Co., Ltd, Changchun, China); and insulin (INS) was determined using an ELISA kit (EIA-2358, Elisa Biotech Co., Ltd. Shanghai, China).

## Determination of Oxidation and Lipid Peroxidation Levels

Serum total superoxide dismutase (SOD), glutathione peroxidase (GSH-Px) and malondialdehyde (MDA) were determined using a SOD assay kit (A001-1, Nanjing Jiancheng Bioengineering Institute, Nanjing, China), an MDA assay kit and a GSH-Px assay kit (A005, Nanjing Jiancheng Bioengineering Institute, Nanjing, China).

Appropriate amounts of hippocampal tissue were weighed and ground with medium, and then the grinding solution was centrifuged. The supernatant was collected to prepare a 10% tissue homogenate. The above kits were used to detect the homogenate.

## Dihydroethidium Staining

Dihydroethylamine (DHE) staining was used to detect the level of ROS in tissues. The brain tissues were removed and sliced into 5-μm paraffin sections by a vibrating slicer as previously described. After washing with phosphate-buffered saline (0.01 M PBS, pH 7.4), the sections were covered with 5 μM DHE (19,709, Kaiman Chemical Co., Ann Arbor, Michigan, USA) and incubated at 37 °C for 30 min under dark conditions. Then, the sections were washed with PBS, covered and observed with a fluorescence microscope. The main fluorescence intensity was calculated in ImageJ software.

## Perls' Staining

After deparaffinization, the sections were washed with PBS and incubated with 3% $H_2O_2$ for 20 min at room temperature. The sections were incubated with Perls' iron reagent containing potassium ferrocyanide and hydrochloric acid for 8 h at 37 °C and rinsed in deionized water. The color of the stained sections was enhanced with a DAB kit (ZLI-9018, ZSGB-BIO, Beijing, China), dehydrated and covered with neutral resin. The mean intensity was calculated in ImageJ software.

## Immunofluorescence Staining

After deparaffinization, the sections were washed with PBS and incubated with 3% $H_2O_2$ for 20 min at room temperature. Then, 0.01 M citrate buffer (pH 6.0) was added to the slices for antigen retrieval, and the slices were blocked with serum. Then, Acyl CoA synthetase long-chain family member 4 (ACSL4, DF12141, Affinity, Cincinnati, OH, USA) and GPX4 (DF6701, Affinity, Cincinnati, OH, USA) were added overnight at 4 °C. After washing with PBS, the sections were incubated with fluorescent secondary antibodies in the dark for 1 h. After washing with PBS, DAPI (2 mg/ml, Solarbio,

Beijing, China) was added, and the sections were incubated for 5 min at room temperature. The brain tissues were covered with antifade mounting medium. The mean intensity was calculated in ImageJ software.

## Western Blot Analysis

Western blot analysis was used to detect protein expression in the hippocampus. First, hippocampal tissues were homogenized in cold RIPA lysis buffer. After centrifugation, the supernatant was collected, and the protein concentration was determined with a BCA protein assay kit (CW0014S, Cwbiotech, Beijing, China). Thirty micrograms of protein was added to a polyacrylamide gel and separated by molecular weight. The separated proteins were transferred onto nitrocellulose filter membranes (NC). The blots were blocked with 5% skim milk and incubated with primary antibodies against GPX4 (DF6701, Affinity, Cincinnati, OH, USA), SCL7A11 (ARG57998, Arigo Biologicals, Shanghai, China), Mitochondrial superoxide dismutase 2, (SOD2, Gb111875, Servicebio, Wuhan, China), L-Ferritin (FTL, ab109373, Abcam, Cambridge, MA, USA), H-Ferritin (FTH, ab183781, Abcam, Cambridge, MA, USA), Transferrin Receptor 1 (TFR, 1,136,890, Invitrogen, Carlsbad, CA, USA), Ferroportin 1 (FPN1, mtp11-a, Alpha Diagnostic International, San Antonio, TX, USA), Mitochondrial Ferritin (Ftmt, ab66111, Abcam, Cambridge, MA, USA), Mitoferrin1 (Mfrn, ab56134, Abcam, Cambridge, MA, USA), Post synaptic density protein 95 (PSD 95, GB11277, Servicebio, Wuhan, China), Synaptophysin (SYN, 17,785–1-AP, Proteintech, Wuhan, China) and Brain-derived neurotrophic factor (BDNF, GB11559, Servicebio, Wuhan, China) overnight at 4 °C. After washing with TBS-T, blots were incubated with HRP-conjugated secondary antibodies, and protein bands were detected by chemiluminescence with a multifunctional laser scanning system (Vilber Fusion FX5 Spectra, Paris, France). The density of protein bands was quantified in ImageJ.

## Statistical Analyses

The results are presented as the mean ± SEM. Statistical comparisons among multiple groups were performed using one-way ANOVA followed by the LSD post hoc test. Two-way ANOVA followed by a Bonferroni post hoc test was used to analyze the behavioral data. $P < 0.05$ was regarded as statistically significant.

# Results

## LIRA Alleviated Disorders of Glycolipid Metabolism and Insulin Resistance in db/db Mice

At the beginning of the experiment, changes in blood glucose were detected weekly in all groups. After LIRA intervention, the elevated blood glucose of db/db mice was significantly improved (Fig. 1A). To study the effects of LIRA on insulin sensitivity and gluconeogenesis, we further evaluated the db/db mouse model by measuring the IPGTT, IPITT and IPPTT levels (Fig. 1B–G). Compared with normal mice, db/db mice demonstrated impaired systemic insulin sensitivity and hepatic gluconeogenesis, which could be reversed by LIRA. Further studies showed that LIRA elicited a decrease in the elevated serum insulin level in db/db mice, which agreed with previous studies

(Fig. 1 H). To gain further insight into the effect of LIRA on lipid metabolism, the serum levels of TC, TG and LDL in mice were further examined. It was not unexpected that the high levels of serum TG and LDL in mice could be reversed by LIRA, but there was no significant difference in the improvement of TC (Fig. 1I–K). In light of the excellent effects from the above in vivo studies, LIRA was demonstrated to significantly improve abnormal glycolipid metabolism and insulin resistance in db/db mice, as we proved again.

## LIRA Attenuated Neurocognitive Deficiencies in db/db Mice

MWM, as a widely used behavioral experiment reflecting cognitive ability, was selected to examine the spatial learning and memory ability of mice. The escape latency and distance during the water maze test were
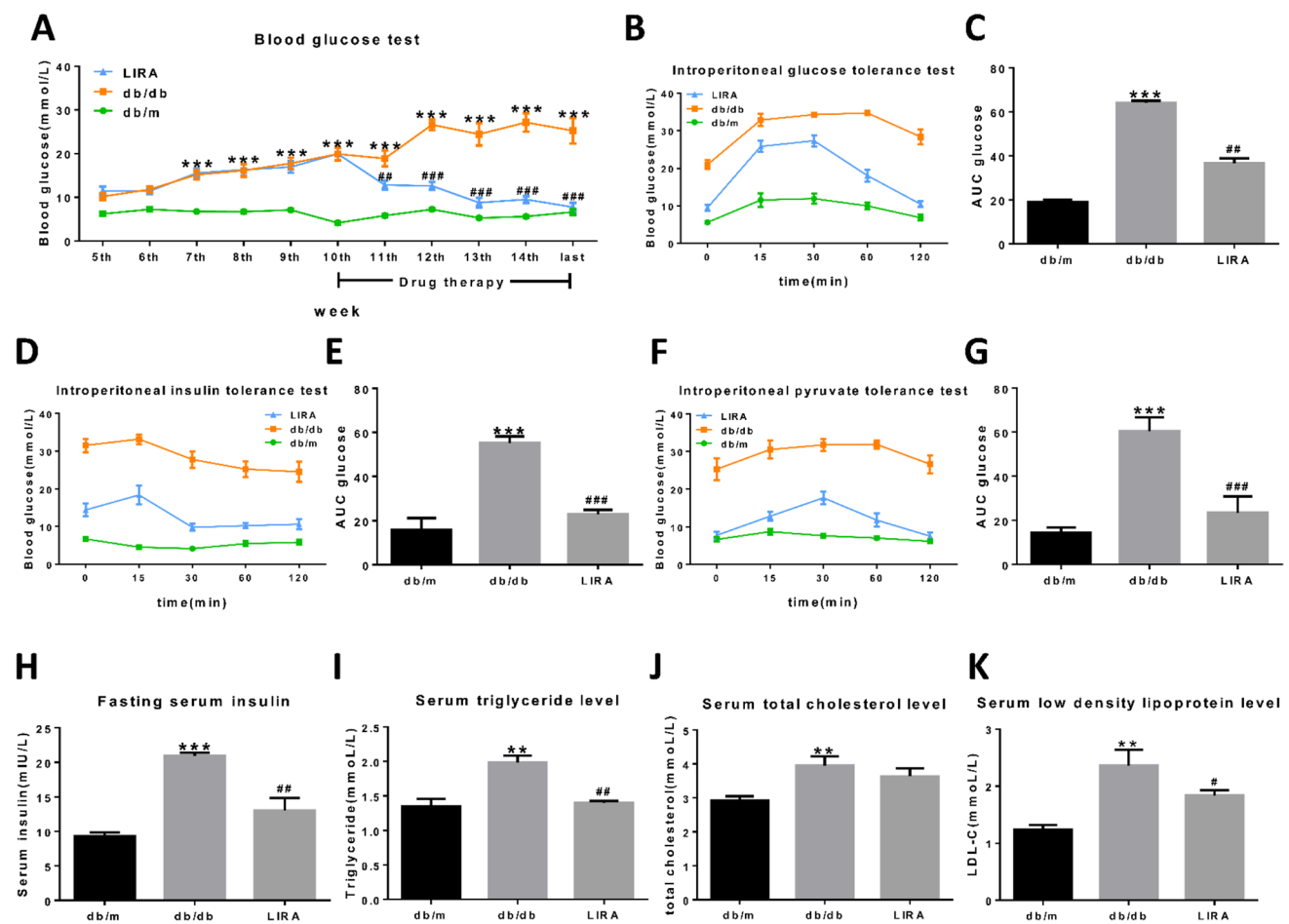


**Fig. 1** Effects of LIRA on glucose and lipid metabolism in db/db mice. **A** Weekly blood glucose test value. **B–G** Intraperitoneal glucose tolerance test (2 g/kg), intraperitoneal insulin tolerance test (0.5 U/kg) and intraperitoneal pyruvate tolerance test (2 g/kg), with the area under the curve (AUC) of the glucose offset curve. **H–K** Serum insulin (**H**), triglyceride (**I**), total cholesterol (**J**), and low-density lipoprotein (**K**) levels in mice. The results are presented as the mean ± SEM. (n = 10), $*p < 0.05$, $**p < 0.01$, $***p < 0.001$ vs. the db/m group; $^{\#}p < 0.05$, $^{\#\#}p < 0.01$, $^{\#\#\#}p < 0.001$ vs. the db/db group

markedly increased in db/db mice compared with normal mice. Similarly, the results of the reversal platform test also showed reduced spatial memory. (Fig. 2A-B). On the final day of the experiment, the db/db mice crossed the platform significantly fewer times within 2 min (Fig. 2C). It is worth mentioning that after LIRA intervention, the increased escape latency and distance and the reduced number of platform crosses were all improved (Fig. 2A–C). Meanwhile, we further evaluated the spatial recognition capability behavior by the Y-maze test. As shown in Fig. 2D–F, the percentage of time spent and the distance traveled in the new zone were elevated in db/db mice. LIRA elicited decreases in the spatial exploration and the damage to recognition abilities. All the above findings indicated the restorative effect of LIRA on learning and memory deficits in db/db mice.

## LIRA Diminished the Loss of Hippocampal Neurons and Improved Synaptic Plasticity Impairments in db/db Mice

First, we observed the synapses by TEM. As shown in Fig. 3A, the width of the synaptic cleft was increased and the thickness of the intersynaptic density was significantly decreased in db/db mice, which was improved after administration of LIRA. Second, we observed hippocampal neurons with Nissl staining. As shown in Fig. 3B, C, Nissl staining became lighter in the CA1 and CA3 regions and the dentate gyrus (DG) of db/db mice, along with a decline in the number of Nissl bodies in the above fields. LIRA elicited a significant increase in the loss of Nissl bodies that resulted from neuronal injury.

Next, we observed changes in the expression of synapse-related proteins in hippocampal neurons, which could directly reflect synaptic damage and degeneration. As shown in Fig. 3D, E, the expression of PSD 95 protein in the hippocampus of db/db mice was reduced, which indicated that the formation of mature synapses was hindered. Similarly, SYN, which is involved in regulating short- and long-term synaptic plasticity, was also significantly differentially expressed between the db/m and db/db groups (Fig. 3D, E). In addition, the levels of BDNF in the hippocampus were inhibited in this model (Fig. 3D, E). Compared with the db/db mice, the LIRA group exhibited significant increases in PSD 95, SYN and BDNF protein expression levels (Fig. 3D, E).

Taken together, these results implied that synaptic dysfunction and neuronal damage in db/db mice attenuate hippocampal memory capacity, which could be reversed by LIRA.

## LIRA Improved Oxidative Stress and Lipid Peroxidation in a db/db Mouse Model

Given that abnormalities in glycolipid metabolism trigger the production of ROS and lipid peroxides, we assessed the positive effects of LIRA on oxidative stress and lipid peroxidation in the hippocampus of db/db mice. First, we detected the levels of SOD, MDA and GSH-Px proteins using ELISA kits. The results revealed that the MDA of the serum was at high levels in the db/db group, but SOD and GSH-Px were at low levels. After LIRA intervention, the MDA level was significantly decreased, while the SOD and GSH-Px levels were significantly increased (Fig. 4A–C). Further analysis of the above findings indicated that the expression levels of SOD, MDA, and GSH-Px in the hippocampus and serum of db/db mice were consistent, while LIRA had the same ameliorative effect (Fig. 4D–F). DHE staining showed that the ROS levels were significantly increased in the hippocampus of db/db mice, and the increases were more pronounced in the CA3 region (Fig. 4G, H). The present findings indicated that LIRA intervention decreased ROS levels (Fig. 4G, H). Moreover, SOD2, an essential antioxidant enzyme in the mitochondrial matrix, was decreased in the hippocampus of db/db mice, as shown in Fig. 4I, J. However, compared with the model group, the expression of SOD2 was upregulated by LIRA. The available data showed that the production of ROS and lipid peroxides in the hippocampus induced by abnormal glucose and lipid metabolism was reduced by LIRA, and the antioxidant and antilipid peroxidation abilities were also restored.

## LIRA Lowered the Iron Levels in the Hippocampus of db/db Mice

Overload of iron contributes to ROS and lipid peroxide generation and memory deficiencies. The cognitive impairment caused by diabetes is known to be associated with iron deposition in the brain [22], but the specific mechanism remains unclear. Hence, we measured the content and distribution of Fe with Perls' staining. As shown in Fig. 5A, B, the Fe content was markedly elevated in the CA1, CA3 and DG regions of the hippocampus. Meanwhile, we detected the content of serum iron and revealed that it was compatible with the variation in iron in the brain (Fig. 5 C).

Next, we sought to explore the underlying mechanism by which regulatory proteins regulate iron intake and release. The expression of the iron storage protein FTH was decreased in the hippocampus of the db/db mice, but there was no significant change in the expression of FTL (Fig. 5D, E). TfR1, an iron intake protein, was elevated in the db/db group, while the sole iron-releasing protein FPN1 displayed a downregulating trend (Fig. 5 D, F). In addition, as the iron-storage protein is located in
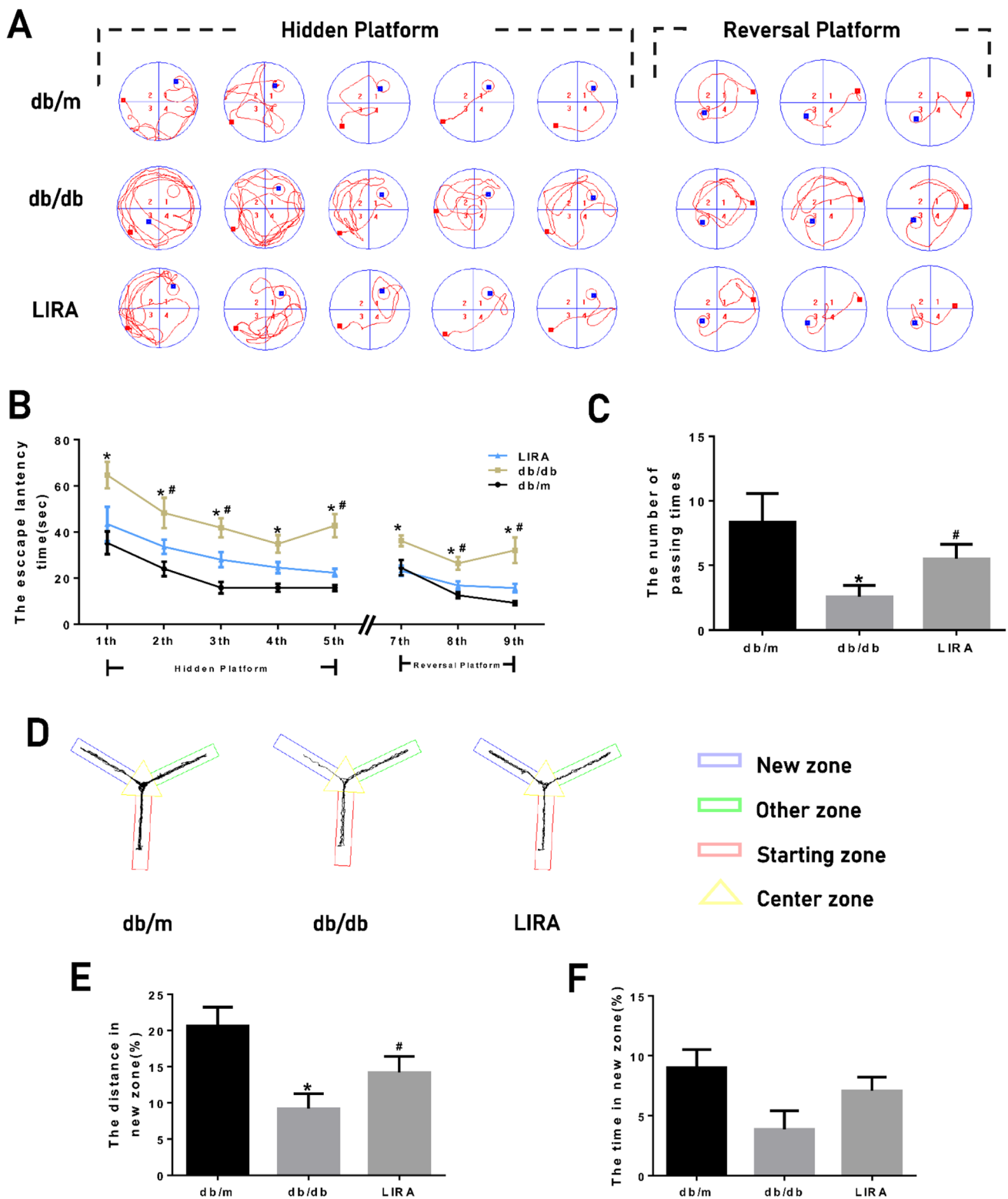
Fig. 2 Morris water maze and Y maze w assessments of LIRA treatment in db/db mice. **A**, **B** The travel distance (m), reversal platform and escape latency (seconds). **C** The times of platform crossing. **D–F** In the Y maze, the ratio of the time percentage and the distance traveled between the starting arms, the new arms and other arms in mice. The results are presented as the mean ± SEM. (n = 10), *$p < 0.05$, **$p < 0.01$, ***$p < 0.001$ vs. the db/m group; #$p < 0.05$, ##$p < 0.01$, ###$p < 0.001$ vs. the db/db group
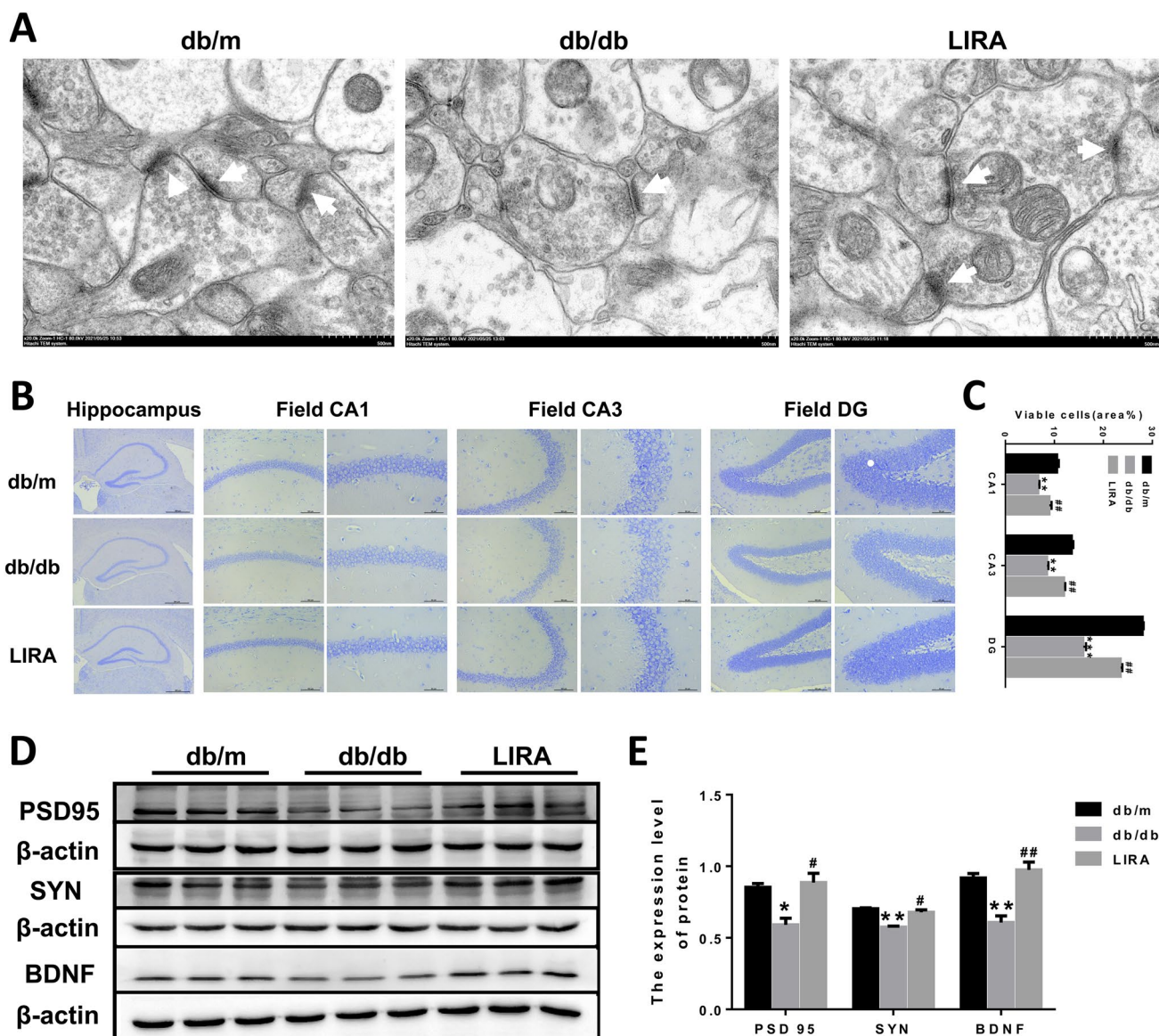
**Fig. 3** The effect of LIRA treatment on neuron and synaptic plasticity in the db/db mouse model. **A** Ultrastructure of hippocampal synapses by TEM (scale bar=50 nm). **B** Nissl staining images from the field CA 1, field CA 3 and the dentate gyrus (DG) at different magnifications (scale bar=500 μm, 100 μm and 50 μm). **C** The number of Nissl substance as shown in the zoom-in images. **D**, **E** The expression and statistical analysis of the PSD 95, SYN and BDNF proteins. The results are presented as the mean±SEM. (n=3), *$p < 0.05$, **$p < 0.01$, ***$p < 0.001$ vs. the db/m group; #$p < 0.05$, ##$p < 0.01$ vs. the db/db group

mitochondria, mitochondrial ferritin (FtMt) was downregulated in db/db mice; conversely, recombinant mitoferrin (Mfrn) was increased (Fig. 5D, G). The findings reported here suggested that LIRA treatment attenuated the increase in Fe content and had a regulatory effect on the levels of proteins representing changes in iron (Fig. 5). Taken together, these observations strongly suggest that db/db mice exhibit iron overload and disordered iron metabolism, which can be rescued by LIRA.

## LIRA Prevented Ferroptosis in the Hippocampus of db/db Mice

Ferroptosis, which differs from other forms of death due to mitochondrial damage, is characterized by smaller mitochondria and increased membrane density [23]. Compared with the db/m group and the LIRA group, the ultrastructural observation of db/db mice showed that the cell volume was reduced, and the mitochondria were reduced and shrunken, which was consistent with the characteristics of ferroptosis

(Fig. 6A). As shown in Fig. 6B, C, the expression of ACSL4 and GPX4 in the rat hippocampal CA3 region was detected by immunofluorescence. The expression level of ACSL4 was increased in the db/db group, whereas GPX4 showed the opposite trend. These findings were more pronounced in the CA3 region. Furthermore, we examined the protein GPX4 and the cystine transporter system protein SLC7A11. The expression of GPX4 was significantly suppressed in db/db mice, and the same trend was observed in SLC7A11 (Fig. 6D, E). Fortunately, these alterations induced by ferroptosis were reversed by LIRA (Fig. 6A–E). Hence, we concluded that ferroptosis can arise in the hippocampus of db/db mice and can be effectively suppressed by LIRA.

## Discussion

This study showed that ferroptosis occurred in the hippocampus of db/db mice; the ferroptosis was manifested by increasing the expression of GPX4 and SLC7A11 and inhibiting excessive ACSL4. In particular, hippocampal oxidative stress, lipid peroxidation, and iron overload caused by diabetes activate ferroptosis, thereby damaging neurons and synaptic plasticity and ultimately causing cognitive dysfunction.

The excellent effects of LIRA on cognitive impairment, as well as on numerous neurodegenerative diseases, have been widely demonstrated, providing greater advantages over other hypoglycemic drugs [24–26]. The ability to improve abnormalities of glycolipid metabolism, as the primary therapeutic benefit of LIRA, is unquestionable. Consistent with previous reports, LIRA significantly improved free choice diet-induced glucose intolerance and reduced hepatic fatty acids, TG, and TC in a novel diet-induced rat obesity model [27]. Similarly, LIRA has been demonstrated to reverse cholesterol transport and improve lipid metabolism and liver lipid accumulation in high fiber diet-fed db/db mice by upregulating ABCA1 expression mediated by ERK1/2 phosphorylation [28]. Once again, our results confirm the stability of this conclusion.

Memory deficit and autonomic behavior are two important roles of hippocampal damage caused by T2DM. Consistent with previous studies, our MWM and Y-maze results showed that diabetic model mice had deficits in spatial learning and memory ability [29, 30]. These results indicate that the db/db mice suffered from impaired long-term and spatial memory functions and exhibited abnormal cognition.

Increasing evidence has suggested that neuronal and synaptic plasticity plays an important role in reflecting learning and memory abilities [31, 32]. Nissl staining has proven to be a reliable marker for neuronal degeneration in the hippocampal CA3 region. As expected, Nissl staining in db/db mice showed significant neuronal loss. Furthermore, transmission electron microscopy indicated impaired synaptic

plasticity, decreased synapses, and thinning of postsynaptic density. At the same time, we detected proteins related to synapses. SYN, a major synaptic vesicle protein, is involved in the structure, function and other membrane components of tissues [33]. It has been reported that high glucose and hypoxia downregulate SYN expression, which may be a potential contributor to cognitive dysfunction in diabetes [34]. PSD 95 is an important scaffolding protein involved in synapse maturation, synapse stability, synaptic transmission, and memory formation in the brain [35]. Previous studies also demonstrated that PSD 95 protein levels in the brain were decreased in STZ-induced hyperglycemic rats, while the expression of PSD 95 could be improved after drug intervention and could subsequently improve long-term synaptic plasticity [36]. BDNF, a member of the neurotrophin family, is of paramount importance in long-term potentiation and neuroplasticity [37]. Previous studies have reported that the distribution and expression of neuronal plasticity markers, including SYN and PSD95, may be modulated by BDNF [38]. Generally, a decrease in BDNF can damage the hippocampus and affect learning and memory function [39], while diabetic rats can cause a significant downregulation of BDNF [36]. Our findings suggested that LIRA could improve the damage and synaptic plasticity of hippocampal neurons in db/db mice, which may be related to the regulation of PSD 95, SYN and BDNF.

Oxidative stress can induce oxidative damage in cells. It has been well established that oxidative stress is involved in the pathogenesis of T2DM, as it is able to induce changes in the morphological and functional changes of brain regions, cause learning and memory impairment, and eventually progress to cognitive impairment [40]. Here, it is worth mentioning that hyperglycemia exerts its stimulatory effect on oxidative stress mainly by increasing the production of mitochondrial ROS, reducing antioxidant SOD and GSH levels, and causing nonenzymatic saccharification of protein and glucose oxidation [41]. Antioxidants that exist in the body can safely interact with free radicals and terminate chain reactions before vital molecules are damaged. Antioxidants can be enzymatic or nonenzymatic, with the former including GSH-Px and SOD and the latter including GSH. The function of SOD is to protect tissue from the deleterious effects of superoxide radicals. GSH-Px can specifically catalyze the reduction of hydroperoxide ($H_2O_2$) to $H_2O$ [41]. The GSH-Px and SOD activities in the brains of db/db mice were markedly decreased. However, after LIRA intervention, the GSH-Px and SOD activities in the mouse brain were restored, which indicated that LIRA shows excellent antioxidant capacity.

Lipid peroxides are considered to be important substances that promote and exacerbate oxidative stress. Lipids (cholesterol, polyunsaturated fatty acids) are the main targets of oxidative attack, which leads to the formation and
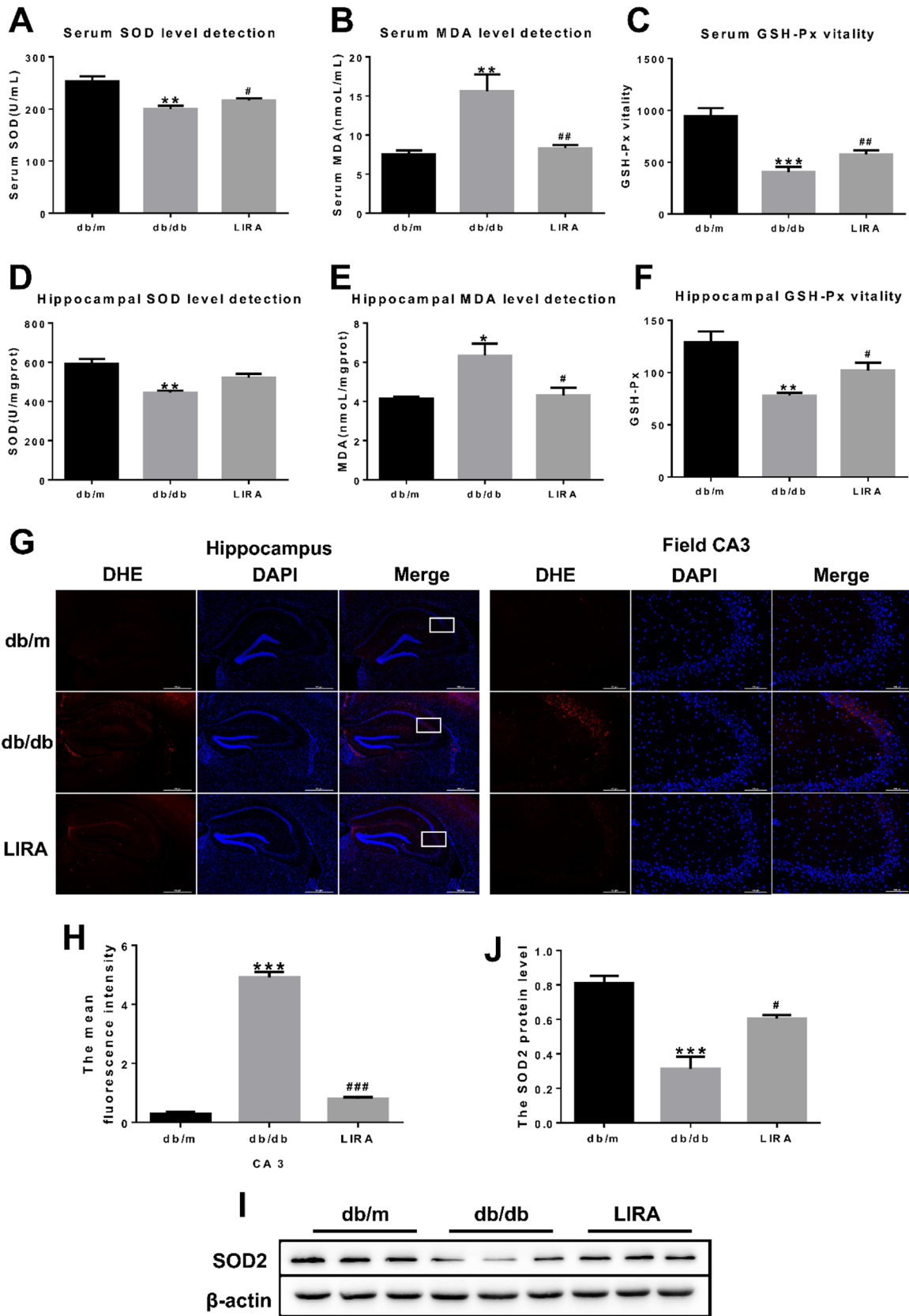
◀**Fig. 4** The expression of oxides and antioxidants in the hippocampus of the db/m, db/db and LIRA groups. **A**–**C** The levels of SOD, MDA and GSH-Px in serum of mice. **D**–**F** The levels of SOD, MDA and GSH-Px in the hippocampus of mice. **G** Image of DHE staining in the field CA3 (scale bar $= 500$ μm, 100 μm and 50 μm). **H** The mean fluorescence intensity as shown in (**G**). **I**, **J** The expression and statistical analysis of the SOD 2 proteins. The results are presented as the mean $\pm$ SEM. n $= 3$, *$p < 0.05$, **$p < 0.01$, ***$p < 0.001$ vs. the db/m group; #$p < 0.05$, ##$p < 0.01$, ###$p < 0.001$ vs. the db/db group

accumulation of lipid oxidation products, particularly oxysterols, hydroperoxides and endoperoxides. The increase in MDA, an important indicator of lipid peroxides, is a special product of lipid peroxidation of the cell membrane during free radical production [42]. Further clinical studies have found that there were high levels of tributyltin compounds, lipid hydroperoxides, and lipid peroxides in the plasma of diabetic individuals [43]. It has been reported that the production of MDA in the hippocampus of db/db mice was increased [44], which was consistent with our results. Likewise, LIRA has a good downregulation effect on MDA, as reported previously [45].

Interestingly, it appears that the CA3 region of the hippocampus is subjected to the most pronounced oxidative attack in the diabetic model. The important role of hippocampal CA3 in long-term memory and spatial working memory has become a consensus, while hippocampal CA3 neurons exhibit disrupted spatial working memory in mice when inhibited from activity [46]. Our results illustrated the more severe damage of the CA3 region in the hippocampus, which might be an important contributor to the impairments of spatial and long-term memory in db/db mice.

Iron is an important trace element. Abnormal homeostasis of iron, such as deficiency or overload, is related to the pathogenesis of various chronic diseases, including diabetes [47]. Several studies have confirmed that the iron content is elevated in diabetes. It has been reported that underexpression of hepcidin in T2DM patients leads to iron overload in the body and triggers the production of reactive oxygen species, which is believed to play a major role in the onset of diabetes mediated by β-cell failure and insulin resistance [48]. Recent reports indicate that the lack of hepcidin in T2DM rats leads to changes in the control of ferroportin and subsequent iron deposition in the hippocampus [49]. Similar to previous reports, our results show that the Fe content was significantly increased, and the iron storage proteins FTL and FTH showed the opposite expression tendency, indicating that db/db mice have increased amounts of free iron in the hippocampus. The expression of Mtft was downregulated, indicating that the accumulation of free iron occurred within mitochondria as well, the center of iron utilization.

TfR1 and FPN1 are important transporters of iron into and out of cells [50], and the main cause of iron deposition is due to higher expression of TfR1 and lower expression of FPN1. For the first time, our results demonstrated that the expression of TfR1 was upregulated and the expression of FPN1 was downregulated in db/db mice. Meanwhile, a similar pattern occurred for Mfrn on mitochondria.

Since excess iron can catalyze hydrogen peroxide into hydroxyl radicals via the Fenton reaction, leading to oxidative stress and lipid peroxidation and inducing neuronal apoptosis [51], iron deposition in the hippocampus can damage cells through oxidative stress and cause cognitive impairment. Pleasingly, LIRA could effectively regulate the expression of iron-related proteins in the hippocampus. Therefore, we speculated that the reduction in iron levels may be an important mechanism of the neuroprotective effects of LIRA (Fig. 7).

Ferroptosis, a regulated and nonapoptotic form of iron-dependent cell death, is characterized by lipid peroxidation on the cell membrane. GPX4, as a key regulatory protein, can convert lipid hydroperoxides into their corresponding lipid alcohols, and this process prevents the iron-dependent formation of toxic lipid ROS and lipid peroxides [52]. Due to GPX4 inactivation and deficient cellular uptake of cysteine, GSH synthesis is insufficient, and the cystine/glutamate antiporter SLC7A11 (xCT) is inhibited, which in turn fails to protect cells from oxidative stress damage [8, 11]. ACSL4, a member of the long-chain family of acyl CoA synthetase proteins, is a key player in metabolism-related diseases and has recently been demonstrated to play an important role in ferroptosis [53]. ACSL4 catalyzes the incorporation of CoA into the long-chain polyunsaturated bonds of arachidonic acid, thereby promoting the esterification of polyunsaturated fatty acid into phospholipids, further inducing the activation of lipid biosynthesis, and finally the ferroptosis involved in lipid conduction [54].

In our current study, LIRA exerted a protective effect against ferroptosis at the level of these proteins in the hippocampus of db/db mice. The results of western blotting revealed greatly elevated GPX4 along with increased SLC7A11 and decreased ACSL4, which was particularly evident in the CA3 region. Since cystine is an essential biosynthesis precursor to glutathione, the compensation mechanism of cystine contributes to synthesizing more glutathione to resist cell ferroptosis.

Taken together, the aforementioned findings suggest that ferroptosis is involved in neuronal cell death and further leads to cognitive impairment in db/db mice, which may be attributed to increased ROS and lipid peroxidation as well as iron deposition (Fig. 7). Interestingly, we found
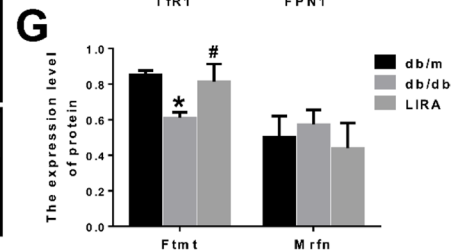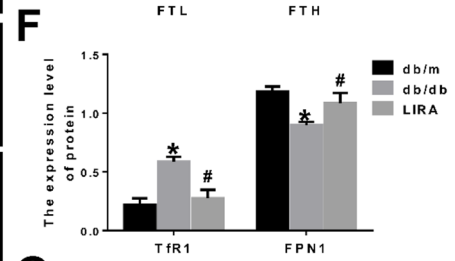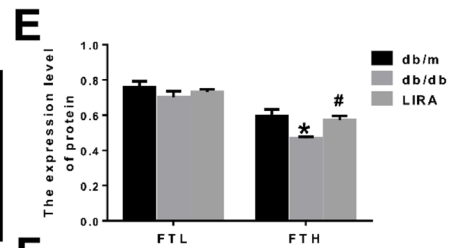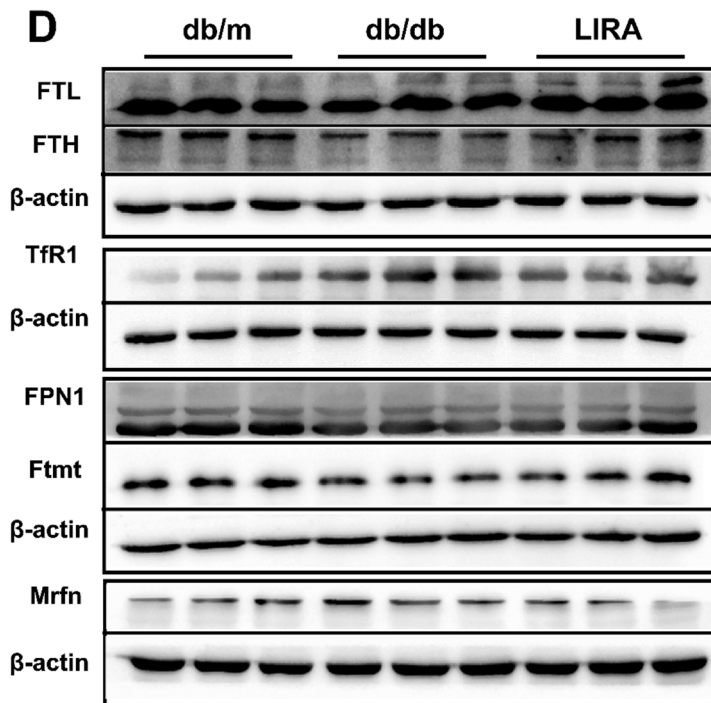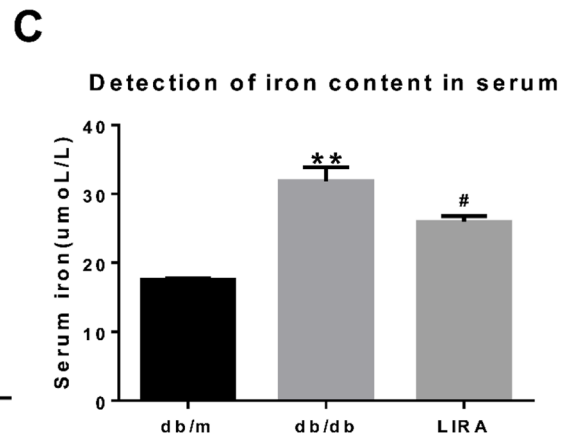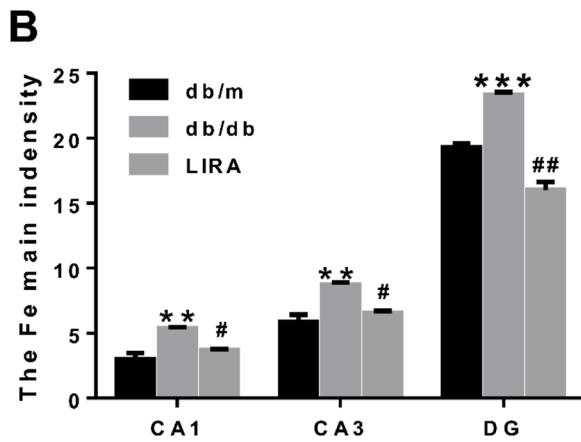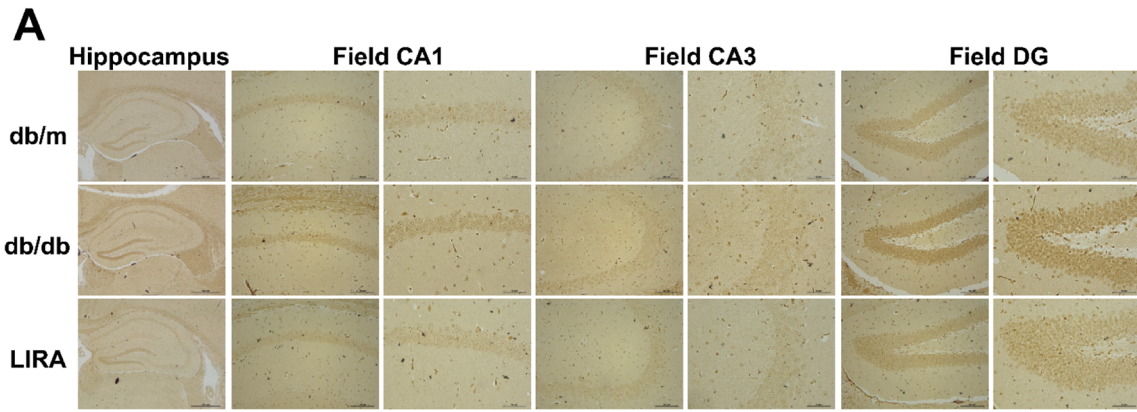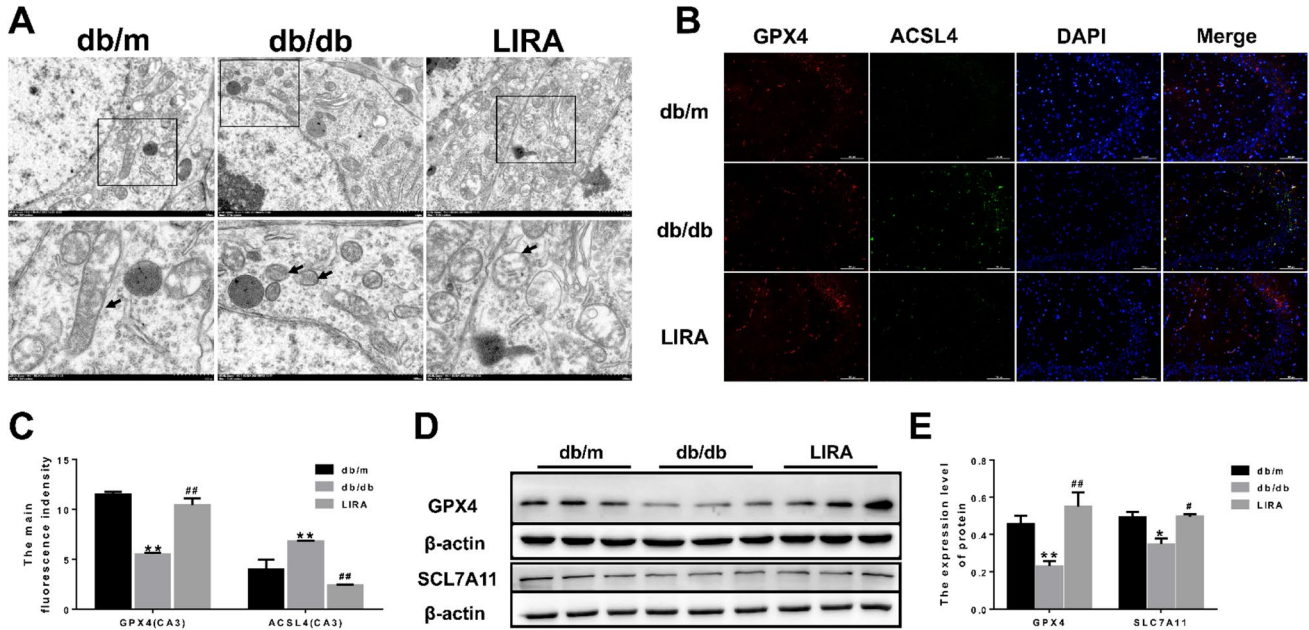
that ferroptosis in hippocampal neurons could be well suppressed. These preliminary findings and related hypotheses need further confirmation and will be the basis of future research on mechanisms involved in LIRA therapy for diabetic cognitive impairment in clinical settings. Moreover, further studies are required to explore the underlying mechanism by which high glucose affects ferroptosis and



**Fig. 6** The effect of LIRA intervention to ferroptosis in the hippocampus of db/db mice. **A** Ultrastructure of mitochondria in the hippocampus by TEM (scale bar = 50 nm). **B**, **C** The GPX 4 and ACSL4 positive cells and DAPI-stained cells in the field CA 3 (scale bar = 500 μm, 100 μm and 50 μm). **D**, **E** The expression and statistical analysis of protein GPX 4 and the protein SLC7A11. The results are presented as the mean ± SEM. n = 3, $*p < 0.05$, $**p < 0.01$ vs. the db/m group; $^{\#}p < 0.05$, $^{\#\#}p < 0.01$ vs. the db/db group
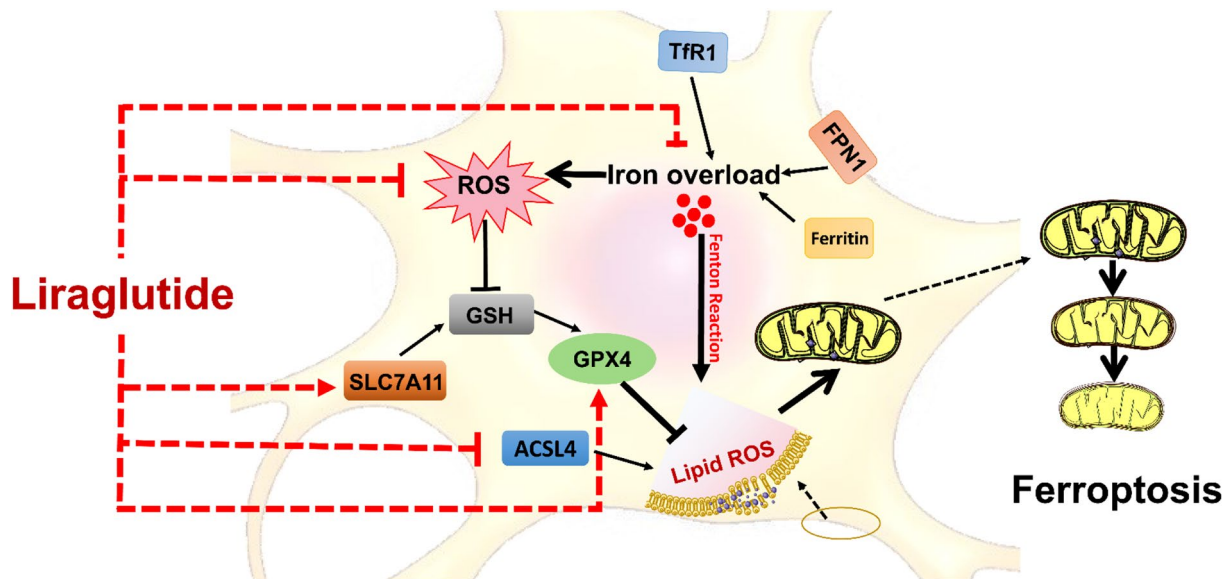


**Fig. 7** The schematic representation of the proposed neuroprotective mechanism of LIRA in the diabetic neurocognitive disorder mimicked by db/db mice. LIRA reduces ferroptosis by suppressing higher oxidative stress and iron levels, further improving hippocampal neuronal and synaptic plasticity, and thereby restoring cognitive impairment in db/db mice

the specific upstream regulatory mechanism of the TfR1/FPN1 protein in T2DM.

## Conclusion

In conclusion, this study shows that LIRA can improve diabetes-induced neuronal damage and synaptic structure and function damage, thereby improving the learning and memory abilities of db/db mice, which may be related to the inhibition of the ferroptosis pathway. In addition, the reduction of oxidative stress and lipid peroxidation and the alleviation of iron overload by LIRA are important reasons for its inhibition of ferroptosis. This provides further reason to continue research on diabetic cognitive impairment and the clinical use of LIRA.

## Declarations

**Ethical Approval** The animal research was approved by the Animal Experimental Ethics Committee of Liaoning University of Traditional Chinese Medicine (Ethics Approval Number: SYXK 2019–0004).

## References

1. Khan MN, Khan FA, Sultana S, Dilawar M, Ijaz A, Khan MJ, Mahmood T (2007) Impact of new diagnostic criteria of diabetes mellitus. J Coll Physicians Surg Pak 17:327–330
2. Anderson RJ, Freedland KE, Clouse RE, Lustman PJ (2001) The prevalence of comorbid depression in adults with diabetes: a meta-analysis. Diabetes Care 24:1069–1078. https://doi.org/10.2337/diacare.24.6.1069
3. Biessels GJ, Strachan MW, Visseren FL, Kappelle LJ, Whitmer RA (2014) Dementia and cognitive decline in type 2 diabetes and prediabetic stages: towards targeted interventions. Lancet Diabetes Endocrinol 2:246–255. https://doi.org/10.1016/S2213-8587(13)70088-3
4. Stoeckel LE, Arvanitakis Z, Gandy S, Small D, Kahn CR, Pascual-Leone A, Pawlyk A, Sherwin R, Smith P (2016) Complex mechanisms linking neurocognitive dysfunction to insulin resistance and other metabolic dysfunction. F1000Res 5:353. https://doi.org/10.12688/f1000research.8300.2
5. Gaspar JM, Baptista FI, Macedo MP, Ambrosio AF (2016) Inside the diabetic brain: role of different players involved in cognitive decline. ACS Chem Neurosci 7:131–142. https://doi.org/10.1021/acschemneuro.5b00240
6. Chatterjee S, Peters SA, Woodward M, Mejia Arango S, Batty GD, Beckett N, Beiser A, Borenstein AR, Crane PK, Haan M, Hassing LB, Hayden KM, Kiyohara Y, Larson EB, Li CY, Ninomiya T, Ohara T, Peters R, Russ TC, Seshadri S, Strand BH, Walker R, Xu W, Huxley RR (2016) Type 2 diabetes as a risk factor for dementia in women compared with men: a pooled analysis of 2.3 million people comprising more than 100,000 cases of dementia. Diabetes Care 39:300–307. https://doi.org/10.2337/dc15-1588
7. Dixon SJ, Lemberg KM, Lamprecht MR, Skouta R, Zaitsev EM, Gleason CE, Patel DN, Bauer AJ, Cantley AM, Yang WS, Morrison B 3rd, Stockwell BR (2012) Ferroptosis: an iron-dependent form of nonapoptotic cell death. Cell 149:1060–1072. https://doi.org/10.1016/j.cell.2012.03.042
8. Sui X, Zhang R, Liu S, Duan T, Zhai L, Zhang M, Han X, Xiang Y, Huang X, Lin H, Xie T (2018) RSL3 drives ferroptosis through GPX4 inactivation and ROS production in colorectal cancer. Front Pharmacol 9:1371. https://doi.org/10.3389/fphar.2018.01371
9. Sumneang N, Siri-Angkul N, Kumfu S, Chattipakorn SC, Chattipakorn N (2020) The effects of iron overload on mitochondrial function, mitochondrial dynamics, and ferroptosis in cardiomyocytes. Arch Biochem Biophys 680:108241. https://doi.org/10.1016/j.abb.2019.108241
10. Lei P, Bai T, Sun Y (2019) Mechanisms of ferroptosis and relations with regulated cell death: a review. Front Physiol 10:139. https://doi.org/10.3389/fphys.2019.00139
11. Stockwell BR, Friedmann Angeli JP, Bayir H, Bush AI, Conrad M, Dixon SJ, Fulda S, Gascon S, Hatzios SK, Kagan VE, Noel K, Jiang X, Linkermann A, Murphy ME, Overholtzer M, Oyagi A, Pagnussat GC, Park J, Ran Q, Rosenfeld CS, Salnikow K, Tang D, Torti FM, Torti SV, Toyokuni S, Woerpel KA, Zhang DD (2017) Ferroptosis: a regulated cell death nexus linking metabolism, redox biology, and disease. Cell 171:273–285. https://doi.org/10.1016/j.cell.2017.09.021
12. Abdul Y, Li W, Ward R, Abdelsaid M, Hafez S, Dong G, Jamil S, Wolf V, Johnson MH, Fagan SC, Ergul A (2021) Deferoxamine treatment prevents post-stroke vasoregression and neurovascular unit remodeling leading to improved functional outcomes in type 2 male diabetic rats: role of endothelial ferroptosis. Transl Stroke Res 12:615–630. https://doi.org/10.1007/s12975-020-00844-7
13. Koekkoek PS, Kappelle LJ, van den Berg E, Rutten GE, Biessels GJ (2015) Cognitive function in patients with diabetes mellitus: guidance for daily care. Lancet Neurol 14:329–340. https://doi.org/10.1016/S1474-4422(14)70249-2
14. Gold SM, Dziobek I, Sweat V, Tirsi A, Rogers K, Bruehl H, Tsui W, Richardson S, Javier E, Convit A (2007) Hippocampal damage and memory impairments as possible early brain complications of type 2 diabetes. Diabetologia 50:711–719. https://doi.org/10.1007/s00125-007-0602-7
15. Inzucchi SE, Bergenstal RM, Buse JB, Diamant M, Ferrannini E, Nauck M, Peters AL, Tsapas A, Wender R, Matthews DR (2012) Management of hyperglycaemia in type 2 diabetes: a patient-centered approach. Position statement of the American Diabetes Association (ADA) and the European Association for the Study of Diabetes (EASD). Diabetologia 55:1577–1596. https://doi.org/10.1007/s00125-012-2534-0
16. Buse JB, Rosenstock J, Sesti G, Schmidt WE, Montanya E, Brett JH, Zychma M, Blonde L, Group L-S (2009) Liraglutide once a day versus exenatide twice a day for type 2 diabetes: a 26-week randomised, parallel-group, multinational, open-label trial

(LEAD-6). Lancet 374:39–47. https://doi.org/10.1016/S0140-6736(09)60659-0

17. Holscher C (2012) Potential role of glucagon-like peptide-1 (GLP-1) in neuroprotection. CNS Drugs 26:871–882. https://doi.org/10.2165/11635890-000000000-00000

18. Hansen HH, Fabricius K, Barkholt P, Niehoff ML, Morley JE, Jelsing J, Pyke C, Knudsen LB, Farr SA, Vrang N (2015) The GLP-1 receptor agonist liraglutide improves memory function and increases hippocampal CA1 neuronal numbers in a senescence-accelerated mouse model of Alzheimer's disease. J Alzheimers Dis 46:877–888. https://doi.org/10.3233/JAD-143090

19. Yuan P, Ma D, Gao X, Wang J, Li R, Liu Z, Wang T, Wang S, Liu J, Liu X (2020) Liraglutide ameliorates erectile dysfunction via regulating oxidative stress, the RhoA/ROCK pathway and autophagy in diabetes mellitus. Front Pharmacol 11:1257. https://doi.org/10.3389/fphar.2020.01257

20. Hayden MR (2019) Type 2 diabetes mellitus increases the risk of late-onset Alzheimer's disease: ultrastructural remodeling of the neurovascular unit and diabetic gliopathy. Brain Sci. https://doi.org/10.3390/brainsci9100262

21. An JR, Zhao YS, Luo LF, Guan P, Tan M, Ji ES (2020) Huper-zine A, reduces brain iron overload and alleviates cognitive deficit in mice exposed to chronic intermittent hypoxia. Life Sci 250:117573. https://doi.org/10.1016/j.lfs.2020.117573

22. Yang Q, Zhou L, Liu C, Liu D, Zhang Y, Li C, Shang Y, Wei X, Li C, Wang J (2018) Brain iron deposition in type 2 diabetes mellitus with and without mild cognitive impairment-an in vivo susceptibility mapping study. Brain Imaging Behav 12:1479–1487. https://doi.org/10.1007/s11682-017-9815-7

23. Maiorino M, Conrad M, Ursini F (2018) GPx4, lipid peroxidation, and cell death: discoveries, rediscoveries, and open issues. Antioxid Redox Signal 29:61–74. https://doi.org/10.1089/ars.2017.7115

24. Femminella GD, Frangou E, Love SB, Busza G, Holmes C, Ritchie C, Lawrence R, McFarlane B, Tadros G, Ridha BH, Bannister C, Walker Z, Archer H, Coulthard E, Underwood BR, Prasanna A, Koranteng P, Karim S, Junaid K, McGuinness B, Nilforooshan R, Macharouthu A, Donaldson A, Thacker S, Russell G, Malik N, Mate V, Knight L, Kshemendran S, Harrison J, Holscher C, Brooks DJ, Passmore AP, Ballard C, Edison P (2019) Evaluating the effects of the novel GLP-1 analogue lira-glutide in Alzheimer's disease: study protocol for a randomised controlled trial (ELAD study). Trials 20:191. https://doi.org/10.1186/s13063-019-3259-x

25. He W, Wang H, Zhao C, Tian X, Li L, Wang H (2020) Role of liraglutide in brain repair promotion through Sirt1-mediated mito-chondrial improvement in stroke. J Cell Physiol 235:2986–3001. https://doi.org/10.1002/jcp.29204

26. Tu XK, Chen Q, Chen S, Huang B, Ren BG, Shi SS (2021) GLP-1R agonist liraglutide attenuates inflammatory reaction and neu-ronal apoptosis and reduces early brain injury after subarachnoid hemorrhage in rats. Inflammation 44:397–406. https://doi.org/10.1007/s10753-020-01344-4

27. Briand F, Brousseau E, Maupoint J, Dubroca C, Costard C, Brey-ner N, Burcelin R, Sulpice T (2020) Liraglutide shows superior cardiometabolic benefits than lorcaserin in a novel free choice diet-induced obese rat model. Eur J Pharmacol 882:173316. https://doi.org/10.1016/j.ejphar.2020.173316

28. Feng WH, Bi Y, Li P, Yin TT, Gao CX, Shen SM, Gao LJ, Yang DH, Zhu DL (2019) Effects of liraglutide, metformin and gli-clazide on body composition in patients with both type 2 diabetes and non-alcoholic fatty liver disease: a randomized trial. J Diabetes Investig 10:399–407. https://doi.org/10.1111/jdi.12888

29. Wang H, Chen F, Du YF, Long Y, Reed MN, Hu M, Suppirama-niam V, Hong H, Tang SS (2018) Targeted inhibition of RAGE reduces amyloid-beta influx across the blood-brain barrier and improves cognitive deficits in db/db mice. Neuropharmacology 131:143–153. https://doi.org/10.1016/j.neuropharm.2017.12.026

30. Ye T, Meng X, Wang R, Zhang C, He S, Sun G, Sun X (2018) Gastrodin alleviates cognitive dysfunction and depressive-like behaviors by inhibiting ER Stress and NLRP3 inflammasome activation in db/db mice. Int J Mol Sci. https://doi.org/10.3390/ijms19123977

31. Bliss TV, Collingridge GL (1993) A synaptic model of memory: long-term potentiation in the hippocampus. Nature 361:31–39. https://doi.org/10.1038/361031a0

32. Muller D, Nikonenko I, Jourdain P, Alberi S (2002) LTP, memory and structural plasticity. Curr Mol Med 2:605–611. https://doi.org/10.2174/1566524023362041

33. McMahon HT, Bolshakov VY, Janz R, Hammer RE, Siegelbaum SA, Sudhof TC (1996) Synaptophysin, a major synaptic vesicle protein, is not essential for neurotransmitter release. Proc Natl Acad Sci USA 93:4760–4764. https://doi.org/10.1073/pnas.93.10.4760

34. Zhao Y, Li Q, Jin A, Cui M, Liu X (2015) E3 ubiquitin ligase Siah-1 downregulates synaptophysin expression under high glu-cose and hypoxia. Am J Transl Res 7:15–27

35. El-Husseini AE, Schnell E, Chetkovich DM, Nicoll RA, Bredt DS (2000) PSD-95 involvement in maturation of excitatory synapses. Science 290:1364–1368

36. Wang X, Zhao L (2016) Calycosin ameliorates diabetes-induced cognitive impairments in rats by reducing oxidative stress via the PI3K/Akt/GSK-3beta signaling pathway. Biochem Biophys Res Commun 473:428–434. https://doi.org/10.1016/j.bbrc.2016.03.024

37. Tran PV, Fretham SJ, Carlson ES, Georgieff MK (2009) Long-term reduction of hippocampal brain-derived neurotrophic factor activity after fetal-neonatal iron deficiency in adult rats. Pediatr Res 65:493–498. https://doi.org/10.1203/PDR.0b013e31819d90a1

38. Robinet C, Pellerin L (2011) Brain-derived neurotrophic factor enhances the hippocampal expression of key postsynaptic pro-teins in vivo including the monocarboxylate transporter MCT2. Neuroscience 192:155–163. https://doi.org/10.1016/j.neuroscience.2011.06.059

39. Hakansson K, Ledreux A, Daffner K, Terjestam Y, Bergman P, Carlsson R, Kivipelto M, Winblad B, Granholm AC, Moham-med AK (2017) BDNF responses in healthy older persons to 35 minutes of physical exercise, cognitive training, and mindfulness: associations with working memory function. J Alzheimers Dis 55:645–657. https://doi.org/10.3233/JAD-160593

40. Xie Y, Chu A, Feng Y, Chen L, Shao Y, Luo Q, Deng X, Wu M, Shi X, Chen Y (2018) MicroRNA-146a: a comprehensive indica-tor of inflammation and oxidative stress status induced in the brain of chronic T2DM rats. Front Pharmacol 9:478. https://doi.org/10.3389/fphar.2018.00478

41. Wu W, Wang X, Xiang Q, Meng X, Peng Y, Du N, Liu Z, Sun Q, Wang C, Liu X (2014) Astaxanthin alleviates brain aging in rats by attenuating oxidative stress and increasing BDNF levels. Food Funct 5:158–166. https://doi.org/10.1039/c3fo60400d

42. Zhong SZ, Ge QH, Qu R, Li Q, Ma SP (2009) Paeonol attenuates neurotoxicity and ameliorates cognitive impairment induced by d-galactose in ICR mice. J Neurol Sci 277:58–64. https://doi.org/10.1016/j.jns.2008.10.008

43. Martin-Gallan P, Carrascosa A, Gussinye M, Dominguez C (2003) Biomarkers of diabetes-associated oxidative stress and antioxidant status in young diabetic patients with or without subclinical com-plications. Free Radic Biol Med 34:1563–1574. https://doi.org/10.1016/s0891-5849(03)00185-0

44. Zhang SY, Ji SX, Bai XM, Yuan F, Zhang LH, Li J (2019) L-3-n-butylphthalide attenuates cognitive deficits in db/db diabetic mice. Metab Brain Dis 34:309–318. https://doi.org/10.1007/s11011-018-0356-6

45. Hussein AM, Eldosoky M, El-Shafey M, El-Mesery M, Abbas KM, Ali AN, Helal GM, Abulseoud OA (2019) Effects of GLP-1 receptor activation on a pentylenetetrazole-kindling rat model. Brain Sci. https://doi.org/10.3390/brainsci9050108

46. Song D, Wang D, Yang Q, Yan T, Wang Z, Yan Y, Zhao J, Xie Z, Liu Y, Ke Z, Qazi TJ, Li Y, Wu Y, Shi Q, Lang Y, Zhang H, Huang T, Wang C, Quan Z, Qing H (2020) The lateralization of left hippocampal CA3 during the retrieval of spatial working memory. Nat Commun 11:2901. https://doi.org/10.1038/s41467-020-16698-4

47. Wilson JG, Lindquist JH, Grambow SC, Crook ED, Maher JF (2003) Potential role of increased iron stores in diabetes. Am J Med Sci 325:332–339. https://doi.org/10.1097/00000441-200306000-00004

48. Ambachew S, Biadgo B (2017) Hepcidin in iron homeostasis: diagnostic and therapeutic implications in type 2 diabetes mellitus patients. Acta Haematol 138:183–193. https://doi.org/10.1159/000481391

49. Liu J, Hu X, Xue Y, Liu C, Liu D, Shang Y, Shi Y, Cheng L, Zhang J, Chen A, Wang J (2020) Targeting hepcidin improves cognitive impairment and reduces iron deposition in a diabetic rat model. Am J Transl Res 12:4830–4839

50. Moos T, Rosengren Nielsen T, Skjorringe T, Morgan EH (2007) Iron trafficking inside the brain. J Neurochem 103:1730–1740. https://doi.org/10.1111/j.1471-4159.2007.04976.x

51. Zhao Y, Xin Z, Li N, Chang S, Chen Y, Geng L, Chang H, Shi H, Chang YZ (2018) Nano-liposomes of lycopene reduces ischemic brain damage in rodents by regulating iron metabolism. Free Radic Biol Med 124:1–11. https://doi.org/10.1016/j.freeradbiomed.2018.05.082

52. Zou MJ, Palte AA, Deik H, Li JK, Eaton W, Wang YY, Tseng R, Deasy M, Kost-Alimova V, Dancik ES, Leshchiner VS, Viswanathan S, Signoretti TK, Choueiri JS, Boehm BK, Wagner JG, Doench CB, Clish PA, Clemons SL (2019) Schreiber, A GPX4-dependent cancer cell state underlies the clear-cell morphology and confers sensitivity to ferroptosis. Nat Commun 10:1617. https://doi.org/10.1038/s41467-019-09277-9

53. Killion EA, Reeves AR, El Azzouny MA, Yan QW, Surujon D, Griffin JD, Bowman TA, Wang C, Matthan NR, Klett EL, Kong D, Newman JW, Han X, Lee MJ, Coleman RA, Greenberg AS (2018) A role for long-chain acyl-CoA synthetase-4 (ACSL4) in diet-induced phospholipid remodeling and obesity-associated adipocyte dysfunction. Mol Metab 9:43–56. https://doi.org/10.1016/j.molmet.2018.01.012

54. Chen X, Li J, Kang R, Klionsky DJ, Tang D (2020) Ferroptosis: machinery and regulation. Autophagy. https://doi.org/10.1080/15548627.2020.1810918

**Publisher's Note** Springer Nature remains neutral with regard to jurisdictional claims in published maps and institutional affiliations.